https://doi.org/10.1080/00150517.2025.2491987

HOW DOES MULTICELLULAR LIFE HAPPEN? MODELING FIBONACCI PATTERNS IN BIOLOGICAL TISSUES UNVEILS UNDERLYING MECHANISMS

BRUCE M. BOMAN

ABSTRACT. The ability of organisms to precisely organize cells in their tissues has allowed multicellular life to exist on earth for hundreds of millions of years. Still, how the cell organization happens remains an enigma. The mechanisms may lie hidden within Fibonacci patterns because many biological tissues have a geometric structure defined by the Fibonacci recurrence relations. Accurate quantitative data describing Fibonacci patterns and their corresponding divergence angles in tissues provides a unique opportunity to uncover the underlying mechanisms. In biology, tissue organization initially arises in stem cell niches that generate circular histological structures. Accordingly, a model for age-structured Fibonacci circle pattern formation was created. Results on order of cell divisions and cyclical pattern growth fit the known biological Fibonacci patterns. Modeling shows that stem cell niche size and specific mode of asymmetric cell division determine the organization of multicellular tissues. It also helps explain how cells organize to form body parts and ultimately a whole organism during development. This mechanism also has important significance for understanding wound healing, tumorigenesis, and birth defects.

KEYWORDS. Fibonacci patterns; tissue organization; stem cell niches; asymmetric cell division; biological modeling

1. INTRODUCTION

Over the last billion years, multicellular life evolved as tissue structure became more and more organized [19]. This raises the question: If multicellular organisms exist because of the precise organization of cells in their tissues, what are the cells doing to form the organized structures? Furthermore, the question—how cell organization happens in tissues?—is even more complex when one realizes that tissue organization is not a static process. Rather, it is extremely dynamic with the organization remaining unchanged while the tissue is continually undergoing renewal by continuous cell division occurring within the tissue itself. Moreover, the biological rules for the organization of tissue structures found in multicellular organisms likely occurred early in evolution. These rules would then be conserved during continued development of higher forms of multicellular organisms. Indeed, the role of pre-existing biological rules as being a determinant along evolutionary paths is well-established. However, the evidence is primarily based on evolutionary trajectories found in anatomic features and not cellular features. For example, the inborn anatomic trait of having five digits (pentadactyly) on limbs occurs across many species [8]. Further anatomic evidence of path-dependent evolution was recently

discovered in the eyes of mollusks [28]. Still, as anyone who has taken a class in plant or animal histology knows, tissue organization is often highly conserved across many different species. Thus, the fundamental rules for cellular organization in tissues still likely exist today in tissues of plants and animals. My goal herein is to study Fibonacci tissue patterns that commonly occur in nature to identify the mathematical laws that describe the cellular rules in biology which explain where the tissue organization comes from.

A key feature of tissue organization is that many histologic structures in biology have a geometric pattern that are described by Fibonacci sequences. In fact, Fibonacci patterns are so widespread in nature [1, 11, 23], the mechanism for tissue organization is likely hidden in the Fibonacci patterns. In plants, Fibonacci numbers often appear in the number of petals on flowers, spirals on a sunflower, or spirals on a pine cone [22, 27]. In animals, Fibonacci numbers are readily observed in tissue patterns found on the nautilus shell, starfish, hydra, and jellyfish [14]. Studies on these geometric structures have produced vast amounts of accurate quantitative data that describe Fibonacci number patterns and their associated divergence angles. While important research has already been done in phyllotaxis to quantitatively describe Fibonacci patterns [1, 11, 22, 26], the mechanisms that explain how the patterns occur in tissues are elusive. So, by modeling Fibonacci patterns, it may be possible to discover the mathematical laws that explain the biologic rules which control tissue organization in multicellular organisms. To begin to address this goal, we previously designed mathematical models based on rules for cell division to see if they might elucidate Fibonacci pattern formation.

In our studies [5, 6, 7], we explored how asymmetric cell division might control the growth and renewal of tissues in multicellular organisms and give rise to the patterns of Fibonacci p-numbers. The Fibonacci p-number sequence is given by the recursive relation $F_n = F_{n-1} + F_{n-p-1}$. The Fibonacci p-numbers are often expressed geometrically (Appendix A). In one study, we created a cell division model for tissue organization based on the biology of tissue renewal [6]. This model was built upon the cell maturation concept for asymmetric cell division published in the landmark papers by Spears and Bicknell-Johnson [24, 25]. Based on the process of asymmetric cell division, our model output simulated the dynamic growth of cell populations and generation of hierarchical patterns found in tissues. Importantly, our modeling [6] generated complex dynamic patterns in which organization of cells in tissues remained constant despite continuous cell division occurring within the tissue structure. In a second study [7], we investigated geometric branching patterns based on Fibonacci p-sequences which revealed how the regularity in branching patterns might occur in biology. This modeling also showed that generation of branching structures produces patterns of self-similarities that occur across different degrees of branching and multiple dimensions. In a third study, I investigated the organization of coverings of geometric capitula and their properties including the angle of rotation which produces a spiral pattern [5]. In that study, different geometric patterns were generated based on the generalized golden p-sections, which are linked to the Fibonacci p-numbers. Modeling showed that generation of various geometric structures have different efficiencies of covering and that regular organizational patterns occur across different golden p-proportions. Therefore, by modeling the spatial and temporal asymmetries of cell division, we discovered that simple biological rules begin

to explain how tissue organization and geometric patterns are maintained in multicellular organisms.

The current study builds upon these previous studies to identify the cellular mechanisms in the stem cell niche and meristem that control tissue organization. Accordingly, I investigated Fibonacci sequence patterns that lead to specific cyclical structures and see if they fit with known Fibonacci patterns and divergence angles in plants and animals. Clearly, available data on the precise organization of different meristems and the accurate quantitative measurements of the divergence angles [11, 12, 15, 16, 20] provides a unique opportunity to create models to uncover the underlying mechanisms.

2. Biology of the Meristem

In biology, the initial step in formation of organized tissues occurs in the meristem or stem cell niche which provides the blueprint from which the tissue structure arises [9]. Specifically, the process starts with a stem cell that, through one or more of its cell divisions, generates offspring cell populations that form ring or circular structures. In plants, some have only one initial cell which gives rise to the whole plant. Others have a group of initial cells rather than just a single initial cell. In the earliest stage of tissue development, a definite and precise pattern, termed a primordium, arises on an initial cellular apex. A primordium of any kind is a circular area or disc of tissue which forms in the first to second subdermal layer of an apical meristem and exhibits a relatively high rate of proliferation. A sequential pattern arises through a process of initiation that is cyclical and involves a specific time interval between the initiation of one primordium and that of the next. The pattern is quantified by measuring the divergence angle. The divergence angle is the smaller of the two angles at the center of a transverse section of a growing shoot tip determined by consecutively initiated primordia [11]. It is essential that the divergence angle is precisely maintained in order to preserve the structure and organization of the tissue. The divergence angle is not only key to developing tissues, but it is also likely paramount to the structure of adult tissues because they are continually undergoing renewal during the lifetime of the organism. While geometric pattern generation from the divergence angle that leads to formation of branched and geometric capitulum structures has been extensively described [1, 10, 11, 14, 17, 18, 21, 22, 23, 27, 29], the processes involved in forming circle structures have been understudied. Accordingly, a model was created herein for age-structured Fibonacci circle pattern formation to investigate how the patterns of primordia arise in different tissues based on their known divergence angles and associated Fibonacci numbers [11, 12, 15, 16, 20].

3. Modeling Approach

The age-structured approach to model Fibonacci circles was based on a combination of two models reported in the literature: 1) asymmetric cell division rules according to A.P. Berdyshev, and 2) circular pattern formation and age structure design based on Parkinson's Law. The rules for asymmetric cell division were first reported in 1972 by the Russian mathematician A. P. Berdyshev [4]. He found that Fibonacci numbers could be generated using an age-based structure whereby cells divide according to a set of rules for asymmetric cell division that included production of dead cells. This unique model produced the same number pattern as the original model described in Fibonacci's

original rabbit problem. The difference between the two models lies in the fact that the Berdyshev model has an age structure that resembles the generation of tissue organization in multicellular organisms whereby cells are born, mature, reproduce, and die.

In 1972, another unique model was published in a book by J. M. Holland entitled "Studies in Structure" [9]. Interestingly, Holland's model was based on the rules for circular pattern formation and circumferential growth according to Parkinson's Law for the structure and expansion of a committee in bureaucratic systems (Appendix B). In this model, the formation of Fibonacci circle patterns occurs following an age-structured approach. This model is particularly interesting because it has a growing circular pattern output and many tissues are epithelia which are often tubular in structure. Indeed, tube formation in tissues involves a dynamic cell division process that forms cyclical structures [2, 3]. Thus, to elucidate the cellular mechanisms that might explain how cell organization occurs in tissues, my model incorporated both Berdyshev's age structure concept [4] and Holland's ideas on circular pattern formation [9].

4. Model Design

The dynamics of age-structured Fibonacci circle pattern formation were modeled to simulate the beginning of tissue development that starts in the stem cell niche, which, through one or more stem cell divisions, generates offspring cell populations that form ring or circular structures. Specifically, the rules for age structure incorporate a cell age-label, number of initiating cells, alternating direction of cell division, the order of cell divisions, and the specific number of cell divisions that the offspring cells undergo. The age structure rules for cell proliferation and maturation include: i) Birth occurring in a stem cell niche or meristem; ii) Maturation whereby cells need to mature before they can divide; iii) Reproduction involving the order and direction of cell divisions; iv) Full maturation wherein cell division stops after specific number of divisions. Further details on the rules for modeling tissue pattern formation and growth are outlined below.

(1) **Cell birth.** One or more initiating cells reside in the stem cell niche. When an initiating cell divides, the younger daughter remains in the stem cell niche and the older daughter cell goes on to eventually mature. The number of initiating cells that reside in the stem cell niche is determined by the number of cells that exist before multiple (> 2) cell divisions occur in a single time period. Thus, each system can be thought of as having two growth zones—a stem cell niche or meristem and a proliferating zone in which the division of cells leads to a Fibonacci number pattern.
(2) **Cell maturation.** Daughter cells must mature over a specific time period before they can divide. Specifically, each cell divides after missing a specified number (one or more) of generations after being produced by an initiating cell.
(3) **Cell division.** Upon undergoing maturation, cells divide according to a set number of divisions, order of division, and direction of division. Cell divisions take place with a definite frequency.
(4) **Cell death.** After cells have undergone a specific number of divisions, they die, but are retained within the Fibonacci circle structure.
(5) **Fibonacci circle structure.** Based on the rules above (1–3), the sequence of cell divisions forms a ring or circle that always leads to exactly the same cyclical arrangement. The initial cell(s) in the stem cell niche or meristem that divide to

produce daughter cells gives rise to the whole of the circle structure. Cell division occurs asymmetrically to generate an older daughter and younger daughter cell. Each cell has an age label that is numbered according to the sequence of cell division. Once a cell is numbered, it always keeps that age label. The order of cell divisions gives rise to the number of cells in each of different time periods that fit the various Fibonacci number sequences. As the number of cell divisions increases over time, the Fibonacci circle will expand circumferentially in size. The fraction of the circle circumference that characterizes the divergence angle of cell division varies according to the circle's specific Fibonacci sequence.

(6) **Fit to biological data.** The patterns generated from the sequences of cell divisions were then analyzed for a fit to various Fibonacci sequences and known angles of divergence in tissues.

5. Results

The age-based structure of the model generated output on: i) the order of cell divisions and ii) specific circle patterns that were then analyzed for fit to known Fibonacci sequences and angles of divergence in tissues. Table 1 lists, according to The On-Line Encyclopedia of Integer Sequences (OEIS) number, the known common Fibonacci sequences, anomalous Fibonacci sequences, and Fibonacci p-number sequences, and their corresponding divergence angles. The process to determine if model output fit these data involved a stepwise approach. The first step was to see if, using Berdyshev age-based cell division rules, the specific order of cell division produces a pattern of successive generations of ancestors that fits each of the Fibonacci sequences. It was then determined if these modeling results could be used to derive the angle of divergence as discussed at the end of the Results section.

Table 1. Fibonacci Number Sequences*.

OEIS #		**Divergence Angle**	**Degrees**
	Common Fibonacci Numbers		
A000045	1, 1, 2, 3, 5, 8, 13, 21, 34, 55, 89, 144, 233, 377, 610 ...	0.381	137.5
A000032	2, 1, 3, 4, 7, 11, 18, 29, 47, 76, 123, 199, 322, 521, ...	0.276	99.36
A000285	1, 4, 5, 9, 14, 23, 37, 60, 97, 157, 254, 411, 665, ...	0.217	78
A022095	1, 5, 6, 11, 17, 28, 45, 73, 118, 191, 309, 500, 809, ...	0.178	64.1
A022096	1, 6, 7, 13, 20, 33, 53, 86, 139, 225, 364, 589, 953, ...	0.151	54.4
A022097	1, 7, 8, 15, 23, 38, 61, 99, 160, 259, 419, 678, ...	0.131	47.25
	Anomalous Fibonacci Numbers		
A001060	2, 5, 7, 12, 19, 31, 50, 81, 131, 212, 343, 555, 898, ...	0.419	151.14
A022113	2, 7, 9, 16, 25, 41, 66, 107, 173, 280, 453, 733, ...	0.439	158.15
A022114	2, 9, 11, 20, 31, 51, 82, 133, 215, 348, 563, 911, ...	0.451	162.42
	Fibonacci p-numbers		
A000930	1, 1, 1, 2, 3, 4, 6, 9, 13, 19, 28, 41, 60, 88, 129, 189, ...	0.318	114.5
A003269	1, 1, 1, 1, 2, 3, 4, 5, 7, 10, 14, 19, 26, 36, 50, 69, 95, ...	0.276	99.2
A003520	1, 1, 1, 1, 1, 2, 3, 4, 5, 6, 8, 11, 15, 20, 26, 34, 45, 60, ...	0.245	88.2
A005708	1, 1, 1, 1, 1, 1, 2, 3, 4, 5, 6, 7, 9, 12, 16, 21, 27, 34, 43, ...	0.222	79.9
*The On-Line Encyclopedia of Integer Sequences, https://oeis.org/			

Modeling the common Fibonacci sequences. The age-based structure for the common Fibonacci number sequences was first determined in order to find the order of cell divisions. For example, the tree diagram in Figure 1A shows the successive order

of cell divisions that produces a pattern that progresses over time that fits the generalized Fibonacci sequence (A000045). Once this age-based structure was established, the Fibonacci circle pattern was formulated (Figure 1B) based on the order of cell divisions (Figure 1C). A linear expression for different cell ages (# new cells and # old cells) at each time period was also derived (Figure 1C). Note that linear geometric progressions can also be expressed as a function of new cells (q) generated – see Appendix C.

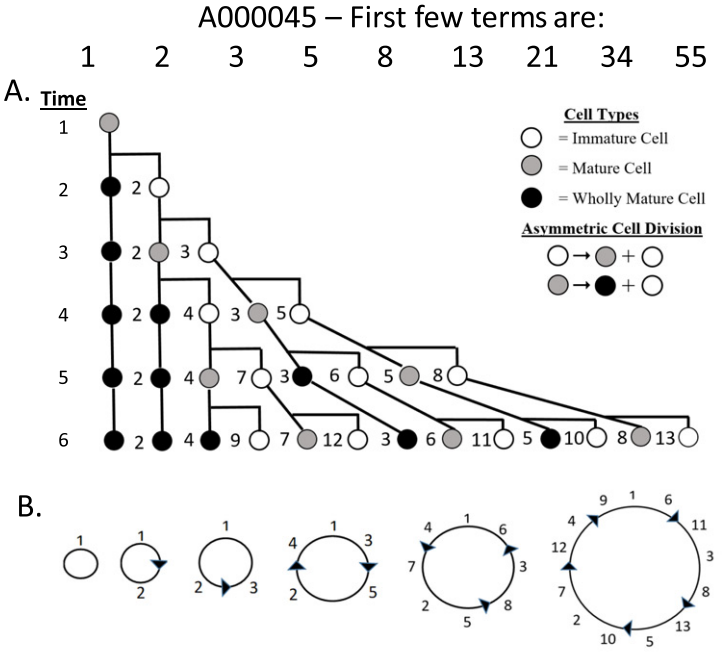

C.

Order of Cell Divisions	1	1→2	2→3	2→4 3→5	3→6 4→7 5→8	4→9 5→10 6→11 7→12 8→13
Linear Expression	1	$q+1$	$q+2$	$2q+3$	$3q+5$	$5q+8$
# Cells	1	2	3	5	8	13

FIGURE 1. The first few terms for the generalized Fibonacci sequence (A000045) are shown. *Panel A*. Modeling was first done, using Berdyshev age-based cell division rules, to find the pattern of successive generations of ancestors that fits the A000045 sequence. Once this age-based structure was established, the Fibonacci circle pattern was formulated (*Panel B*) based on the order of cell divisions (*Panel C*). The successive generation of Fibonacci circle patterns based on the sequence of cell divisions from 1 cell to 13 cells is shown. The linear expressions in terms of cell divisions (q = # new cells from cell division) are also given. For example, at time cycle 6, there are 5 new cells that were generated and 8 cells remained from the previous generation at time cycle 5. Thus a total of 13 cells (5 new and 8 old) are present at time cycle 6.

In a similar manner (see Figure 2), modeling was done to find the order of cell divisions and pattern of successive generations that fits the Lucas number sequence (A000032). Once this order of cell divisions was determined, the Fibonacci circle pattern and linear expression for different cell ages were established for the Lucas number sequence. The order and number of cell divisions was then determined for the other common Fibonacci sequences (Table 2).

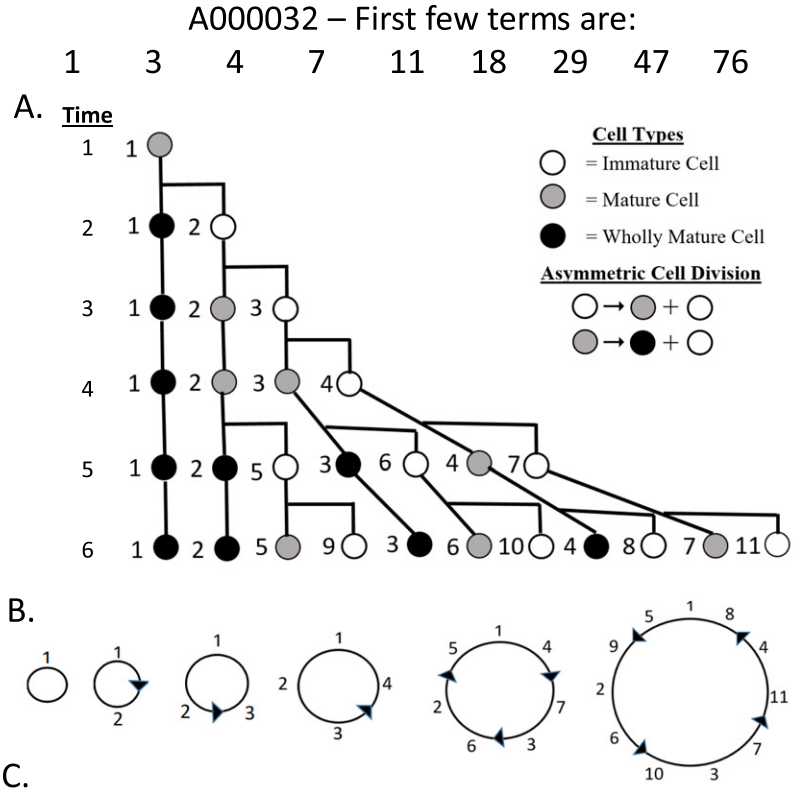

Order of Cell Divisions	1	1→2	2→3	3→4	2→5 3→6 4→7	4→8 5→9 6→10 7→11
Linear Expression	1	$2-q$	$2q+1$	$q+3$	$3q+4$	$4q+7$
# Cells	1	2	3	4	7	11

FIGURE 2. The first few terms for the Lucas number sequence (A000032) are shown. *Panel A*. Modeling was first done, using Berdyshev cell division rules, to find the pattern of successive generations that fits the A000032 sequence. Once this age-based structure was established, it was possible to formulate the Fibonacci circle pattern (*Panel B*) according to the order of cell divisions (*Panel C*). The linear expressions in terms of cell divisions are also given.

Interestingly, the analysis of all the common Fibonacci number sequences produced a particular pattern that emerged across the different sequences. Namely, there is a progressive increase in number of initiating cells that exist before multiple (> 2) cell divisions occur in a single time period (shaded areas in Table 2). Modeling to generate tree structures (using Berdyshev cell division rules) illustrates how this happens (Figure 3).

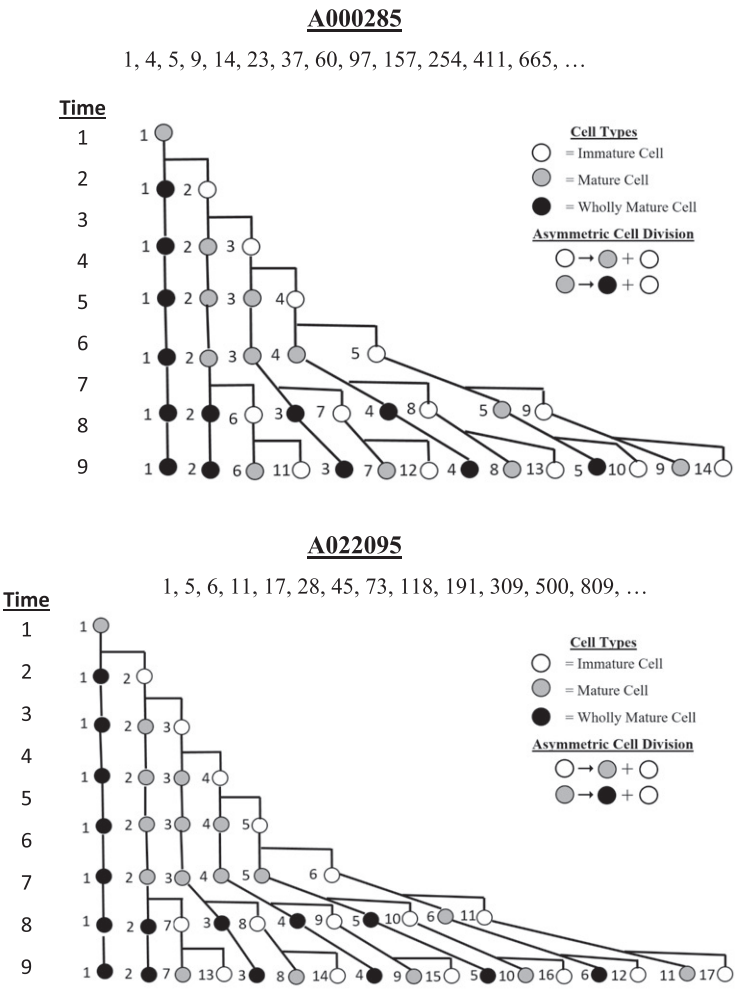

FIGURE 3. The first few terms for two other common Fibonacci number sequences (A000285 and A022095) are shown. Modeling, using the same Berdyshev cell division rules, was able to find the pattern of successive generations that fits these sequences. The difference, however, between the tree age-structures shown in Figure 3 and those structures shown in Figures 1 and 2, is that the number of initiating cells (5 and 6 cells) is greater for structures that fit A000285 and A022095 compared to those (3 and 4 cells) for A000045 and A000032 (Figures 1 and 2). The number of initiating cells that reside in the stem cell niche is determined by the number of cells that exist before multiple (> 2) cell divisions occur in a single time period.

TABLE 2. Order & Number of Cell Divisions for Common Fibonacci Sequences.

	Order of Cell Divisions*					
Time	**A000045**	**A000032**	**A000285**	**A022095**	**A022096**	**A022097**
1	1	1	1	1	1	1
2	1→2	1→2	1→2	1→2	1→2	1→2
3	2→3	2→3	2→3	2→3	2→3	2→3
4	2→4 3→5	3→4	3→4	3→4	3→4	3→4
5	3→6 4→7 5→8	2→5 3→6 4→7	4→5	4→5	4→5	4→5
6	4→9 5→10 6→11 7→12 8→13	4→8 5→9 6→10 7→11	2→6 3→7 4→8 5→9	5→6	5→6	5→6
7	6→14 7→15 8→16 9→17 10→18 11→19 12→20 13→21	5→12 6→13 7→14 8→15 9→16 10→17 11→18	5→10 6→11 7→12 8→13 9→14	2→7 3→8 4→9 5→10 6→11	6→7	6→7
8	9→22 10→23 11→24 12→25 13→26 14→27 15→28 16→29 17→30 18→31 19→32 20→33 21→34	8→19 9→20 10→21 11→22 12→23 13→24 14→25 15→26 16→27 17→28 18→29	6→15 7→16 8→17 9→18 10→19 11→20 12→21 13→22 14→23	6→12 7→13 8→14 9→15 10→16 11→17	2→8 3→9 4→10 5→11 6→12 7→13	7→8

TABLE 2. (*Continued*).

9	•	•	•	7→18		
	•	•	•	8→19		
	•	•	•	9→20	7→14	2→9
	•	•	•	10→21	8→15	3→10
	•	•	•	11→22	9→16	4→11
	•	•	•	12→23	10→17	5→12
	•	•	•	13→24	11→18	6→13
	•	•	•	14→25	12→19	7→14
	•	•	•	15→26	13→20	8→15
	•	•	•	16→27		
	•	•	•	17→28		
*Highlighted areas have only a single cell division at that time period						

Number of Cell Divisions						
Time	**A000045**	**A000032**	**A000285**	**A022095**	**A022096**	**A022097**
1	1	1	1	1	1	1
2	1	-1	1	1	1	1
3	1	2	1	1	1	1
4	2	1	1	1	1	1
5	3	3	1	1	1	1
6	5	4	4	1	1	1
7	8	7	5	5	1	1
8	13	11	9	6	6	1
9	21	18	14	11	7	7

Linear Expressions in Terms of Cell Divisions (q)						
Time	**A000045**	**A000032**	**A000285**	**A022095**	**A022096**	**A022097**
1	1	1	1	1	1	1
2	$q+1$	$2-q$	$q+1$	$q+1$	$q+1$	$q+1$
3	$q+2$	$2q+1$	$q+2$	$q+2$	$q+2$	$q+2$
4	$2q+3$	$q+3$	$q+3$	$q+3$	$q+3$	$q+3$
5	$3q+5$	$3q+4$	$q+4$	$q+4$	$q+4$	$q+4$
6	$5q+8$	$4q+7$	$4q+5$	$q+5$	$q+5$	$q+5$
7	$8q+13$	$7q+11$	$5q+9$	$5q+6$	$q+6$	$q+6$
8	$13q+21$	$11q+18$	$9q+14$	$6q+11$	$6q+7$	$q+7$
9	$21q+34$	$18q+29$	$14q+23$	$11q+17$	$7q+13$	$7q+8$

Specifically, the pattern of successive generations that fits common Fibonacci sequences A000285 and A022095 shows there is a greater number of initiating cells (5 and 6 cells, respectively) compared to the number of initiating cells found for Fibonacci sequences A000045 and A000032 (3 and 4 cells, respectively; Figures 1 and 2). The other common Fibonacci number patterns (A022096 and A022097) show even more initiating cells (Table 2). This finding indicates that there is a different number of initiating cells that reside in the stem cell niche in the different meristems that generate common Fibonacci number patterns. It also suggests that the stem cell niche (i.e., initiating cell number) determines the cellular organization of the meristem. Indeed, a specific Fibonacci circle pattern was found that corresponds to each of the common Fibonacci number sequences (Figure 4).

Representative Fibonacci Circles for Common Fibonacci Number Sequences

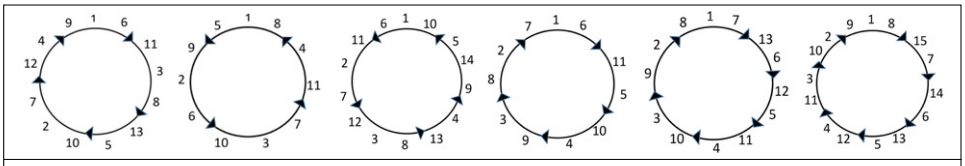

A000045	A000032	A000285	A022095	A022096	A022097
13 cells ($t = 7$)	11 cells ($t = 6$)	14 cells ($t = 5$)	11 cells ($t = 4$)	13 cells ($t = 4$)	15 cells ($t = 4$)

Total Number of Cells												
Time (t)	***1***	***2***	***3***	***4***	***5***	***6***	***7***	***8***	***9***	***10***	***11***	***12***
A000045	1	1	2	3	5	8	13	21	34	55	89	144
A000032	2	1	3	4	7	11	18	29	47	76	123	199
A000285	1	4	5	9	14	23	37	60	97	157	254	411
A022095	1	5	6	11	17	28	45	73	118	191	309	500
A022096	1	6	7	13	20	33	53	86	139	225	364	589
A022097	1	7	8	15	23	38	61	99	160	259	419	678

FIGURE 4. The specific Fibonacci circle patterns that were deduced for each of the common Fibonacci number sequences, A000045, A000032, A000285, A022095, A022096, and A022097, are shown for the indicated cell stages. The number sequences based on Berdyshev cell division rules over time (t) for these common Fibonacci series are shown in the lower Table with the number of cells highlighted that corresponds to the Fibonacci circles shown above.

Modeling the anomalous Fibonacci sequences. The age-based structure for the anomalous Fibonacci sequences was also determined in order to find the order of cell divisions. For example, Figure 5 shows the tree diagram for the pattern of successive generations of ancestors that fits the anomalous sequence A001060 and the Fibonacci circle pattern based on the order of cell division. Figure 6 shows the specific Fibonacci circle patterns that were deduced for each of the anomalous Fibonacci sequences A001060, A022113, and A022114. The order of cell division and the linear expressions in terms of cell divisions for these Fibonacci sequences are given in Table 3. Note that the number of initiating cells is two cells for all of the anomalous Fibonacci sequence patterns. The difference between the age-structure patterns among the three different anomalous Fibonacci sequences lies in the variable number of cell divisions in the third time period after the stem cell niche has formed. Namely, this difference happens because a stem cell and one or more of its daughters divide more than once in the third time period (Figures 5 and 6, Table 3).

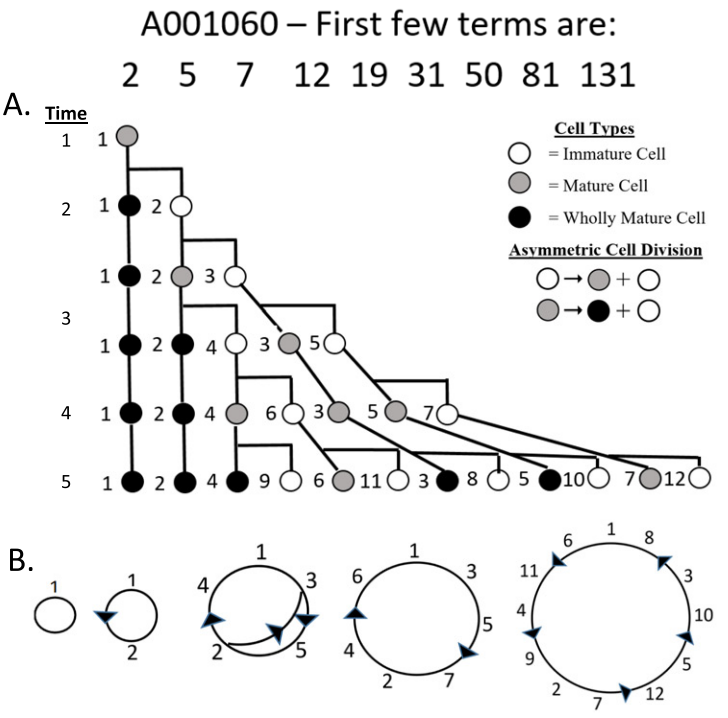

C.

Order of Cell Divisions	1	1→2	2→3 2→4 3→5	4→6 5→7	3→8 4→9 5→10 6→11 7→12
Linear Expression	1	$-q+3$	$3q+2$	$2q+5$	$5q+7$
# Cells	1	2	5	7	12

FIGURE 5. The first few terms for the anomalous Fibonacci sequence A001060 are shown. *Panel A*: The tree diagram shows the pattern of successive generations of ancestors that fits the A001060 sequence as deduced using Berdyshev cell division rules. Once this age-based structure was established, the Fibonacci circle pattern (*Panel B*) was formulated according to the order of cell divisions (*Panel C*). The linear expressions in terms of cell divisions are given in *Panel C*.

TABLE 3. Order & Number of Cell Divisions for Anomalous Fibonacci Sequences.

Order of Cell Divisions*			
Time	**A001060**	**A022113**	**A022114**
1	1	1	1
2	1→2	1→2	1→2
3	2→3 2→4 3→5	2→3 2→4 3→5 4→6 5→7	2→3 2→4 3→5 4→6 5→7 6→8 7→9
4	4→6 5→7	6→8 7→9	8→10 9→11
5	3→8 4→9 5→10 6→11 7→12	3→10 4→11 5→12 6→13 7→14 8→15 9→16	3→12 4→13 5→14 6→15 7→16 8→17 9→18 10→19 11→20
6	6→13 7→14 8→15 9→16 10→17 11→18 12→19	8→17 9→18 10→19 11→20 12→21 13→22 14→23 15→24 16→25	10→21 11→22 12→23 13→24 14→25 15→26 16→27 17→28 18→29 19→30 20→31
*Highlighted areas have only a single cell division at that time period			

Number of Cell Divisions			
Time	**A001060**	**A022113**	**A022114**
1	0	0	0
2	1	1	1
3	3	5	7
4	2	2	2
5	5	7	9
6	7	9	11
7	12	16	20
8	19	25	31
9	31	41	51

TABLE 3. (*Continued*).

Linear Expressions in Terms of Cell Divisions (q)			
Time	**A001060**	**A022113**	**A022114**
1	1	1	1
2	$-q+3$	$q+1$	$q+1$
3	$3q+2$	$5q+2$	$q+2$
4	$2q+5$	$2q+7$	$2q+9$
5	$5q+7$	$7q+9$	$9q+11$
6	$7q+12$	$9q+16$	$11q+20$

Representative Fibonacci Circles for Anomalous Fibonacci Number Sequences

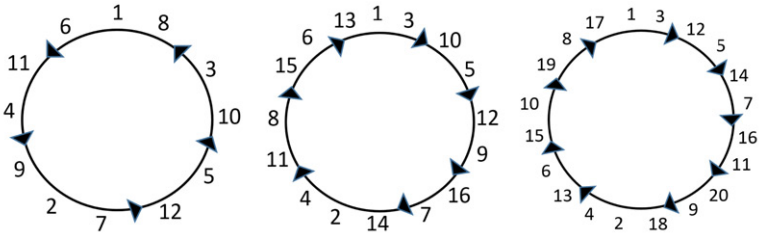

A001060	**A022113**	**A022114**
12 cells (t = 4)	16 cells (t = 4)	20 cells (t = 4)

Time	1	2	3	4	5	6	7	8	9	10	11	12
A001060	2	5	7	12	19	31	50	81	131	212	343	555
A022113	2	7	9	16	25	41	66	107	173	280	453	733
A022114	2	9	11	20	31	51	82	133	215	348	563	911

FIGURE 6. The specific Fibonacci circle patterns that were deduced for each of the anomalous Fibonacci sequences, A001060, A022113, and A022114, are shown for the indicated cell stages. The number sequences [13, 26] based on Berdyshev cell division over time (t) for these anomalous Fibonacci series are shown in the lower Table with the number of cells highlighted that correspond to the Fibonacci circles shown above.

Modeling the Fibonacci p-number sequences. The age-based structure for the Fibonacci p-number sequences was also determined. For example, Figure 7 shows the tree diagram for the pattern of successive generations of ancestors that fits the A000930 sequence and the corresponding Fibonacci circle pattern based on the order of cell divisions. Notably, Figure 7 shows that there is a maturation delay of an extra time cycle for immature cells to develop into mature cells. Rules for changes in the direction of cell division and the specific number of cell divisions that the offspring cells undergo also differ among the different Fibonacci p-number patterns. The specific Fibonacci circle patterns that were deduced for each of the Fibonacci p-number sequences are illustrated in Figure 8. The order of cell division and the linear expressions in terms of cell divisions for these Fibonacci sequences are given in Table 4. Note that the number of initiating cells increases from 4 to 7 cells (shaded area in Table 4) for the Fibonacci p-number sequences patterns.

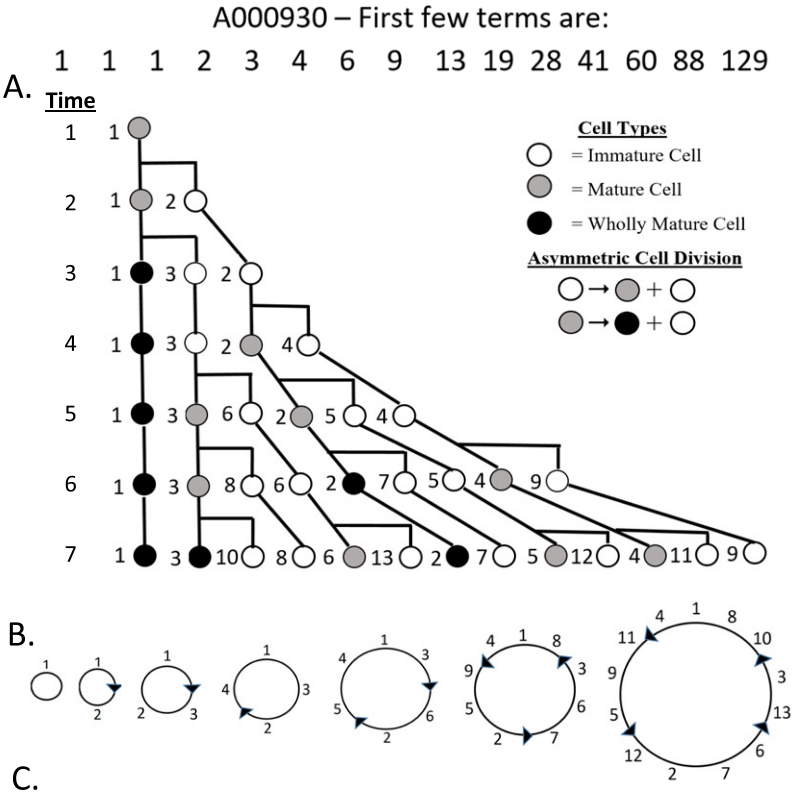

Order of Cell Divisions	1→2	1→3	2→4	2→5 3→6	2→7 3→8 4→9	3→10 4→11 5→12 6→13
Linear Expression	$q+1$	$q+2$	$q+3$	$2q+4$	$3q+6$	$4q+9$
# Cells	2	3	4	6	9	13

FIGURE 7. The first few terms for the Fibonacci p-sequence A000930 are shown. *Panel A*: The tree diagram shows the pattern of successive generations of ancestors that fits the A000930 sequence as deduced using Berdyshev cell division rules. Based on this age-based structure, the Fibonacci circle pattern (*Panel B*) was then formulated according to the order of cell divisions (*Panel C*). The linear expressions in terms of cell divisions are in *Panel C*.

TABLE 4. Order & Number of Cell Divisions for Fibonacci p-Numbers.

Order of Cell Divisions				
Time	**A000930**	**A003269**	**A003520**	**A005708**
1	1	1	1	1
2	1→2	1→2	1→2	1→2
3	1→3	1→3	1→3	1→3
4	2→4	1→4	1→4	1→4
5	2→5 3→6	2→5	1→5	1→5
6	2→7 3→8 4→9	2→6 3→7	2→6	1→6
7	3→10 4→11 5→12 6→13	2→8 3→9 4→10	2→7 3→8	2→7
8	4→14 5→15 6→16 7→17 8→18 9→19	2→11 3→12 4→13 5→14	2→9 3→10 4→11	2→8 3→9
9	5→20 6→21 7→22 8→23 9→24 10→25 11→26 12→27 13→28	3→15 4→16 5→17 6→18 7→19	2→12 3→13 4→14 5→15	2→10 3→11 4→12
10	• • • • • • •	4→20 5→21 6→22 7→23 8→24 9→25 10→26	2→16 3→17 4→18 5→19 6→20	2→13 3→14 4→15 5→16
11	• • • • • •	• • • • • •	3→21 4→22 5→23 6→24 7→25 8→26	2→17 3→18 4→19 5→20 6→21
12	• • • • • •	• • • • • •	• • • • • •	2→22 3→23 4→24 5→25 6→26 7→27

TABLE 4. (*Continued*).

Number of Cell Divisions				
Time	**A000930**	**A003269**	**A003520**	**A005708**
1	1	1	1	1
2	1	1	1	1
3	1	1	1	1
4	1	1	1	1
5	2	1	1	1
6	3	2	1	1
7	4	3	2	1
8	6	4	3	2
9	9	5	4	3
10	13	7	5	4
11	19	10	6	5
12	28	14	8	6
13	41	19	11	7

Linear Expressions in Terms of Cell Divisions (q)				
Time	**A000930**	**A003269**	**A003520**	**A005708**
1	1	1	1	1
2	$q+1$	$q+1$	$q+1$	$q+1$
3	$q+2$	$q+2$	$q+2$	$q+2$
4	$q+3$	$q+3$	$q+3$	$q+3$
5	$2q+4$	$q+4$	$q+4$	$q+4$
6	$3q+6$	$2q+5$	$q+5$	$q+5$
7	$4q+9$	$3q+7$	$2q+6$	$q+6$
8	$6q+13$	$4q+10$	$3q+8$	$2q+7$
9	$9q+19$	$5q+14$	$4q+11$	$3q+9$
10	$13q+28$	$7q+19$	$5q+15$	$4q+12$
11	$19q+41$	$10q+26$	$6q+20$	$5q+16$
12	$28q+60$	$14q+36$	$8q+26$	$6q+21$
13	$41q+88$	$19q+50$	$11q+34$	$7q+27$

Representative Fibonacci Circles for Fibonacci *p*-Number Sequences

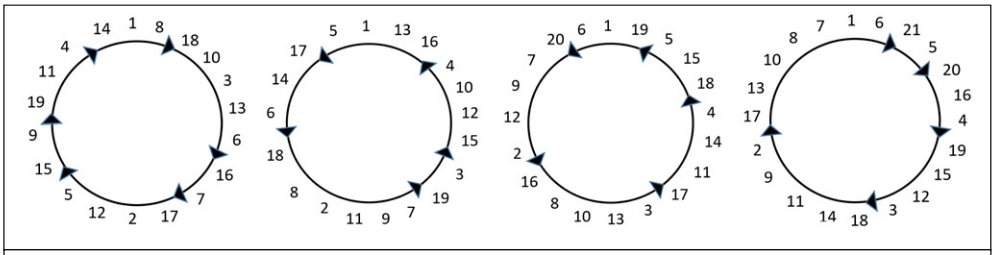

A000930	A003269	A003520	A005708
19 cells (t = 9)	19 cells (t = 12)	20 cells (t = 14)	21 cells (t = 16)

Total Number of Cells																
Time	***1***	***2***	***3***	***4***	***5***	***6***	***7***	***8***	***9***	***10***	***11***	***12***	***13***	***14***	***15***	***16***
A000930	1	1	1	3	4	6	9	13	19	28	41	60	88	129	189	277
A003269	1	1	1	1	2	3	4	5	7	10	14	19	26	36	50	69
A003520	1	1	1	1	1	2	3	4	5	6	8	11	15	20	26	34
A005708	1	1	1	1	1	1	2	3	4	5	6	7	9	12	16	21

FIGURE 8. The specific Fibonacci circle patterns that were deduced for each of the Fibonacci *p*-sequences, A000930, A003269, A003520, and A005708, are shown for the indicated cell stages. The number sequences based on Berdyshev's cell division rules over time (t) for these Fibonacci *p*-sequences are shown in the lower Table with the number of cells highlighted that correspond to the Fibonacci circles shown above.

Modeling the angles of divergence. Once specific age-based structures were found that fit each of the different Fibonacci number sequence patterns, it was determined if these modeling results could be used to derive the angle of divergence that corresponds to each sequence. Indeed, the results show that divergence angles can be derived from the number of cells at successive time cycles (Table 5) and from ratios of the linear expressions (Table 6). Moreover, it was discovered that a linear relation exists between the stem cell niche size, in terms of number of initiating cells, and the divergence angle (Figure 9). The differences in stem cell niche size and rules for cell division among the different Fibonacci number patterns are summarized in Table 7—see below.

TABLE 5. Derivation of the Divergence Angles from Number of Cells at Successive Time Cycles.

OEIS #							Divergence Angle	Degrees
Common Fibonacci Numbers								
A000045	$1/3$	$2/5$	$3/8$	$5/13$	$8/21$	$13/34$	0.381	137.5
A000032	$1/4$	$2/7$	$3/11$	$5/18$	$8/29$	$13/47$	0.276	99.36
A000285	$1/5$	$2/9$	$3/14$	$5/23$	$8/37$	$13/60$	0.217	78
A022095	$1/6$	$2/11$	$3/17$	$5/28$	$8/45$	$13/73$	0.178	64.1
A022096	$1/7$	$2/13$	$3/20$	$5/33$	$8/53$	$13/86$	0.151	54.4
A022097	$1/8$	$2/15$	$3/23$	$5/38$	$8/61$	$13/99$	0.131	47.25
Anomalous Fibonacci Numbers								
A001060	$1/2$	$2/5$	$3/7$	$5/12$	$8/19$	$13/31$	0.419	151.14
A022113	$1/2$	$3/7$	$4/9$	$7/16$	$11/25$	$18/41$	0.439	158.15
A022114	$1/2$	$4/9$	$5/11$	$9/20$	$14/31$	$23/51$	0.451	162.42
Fibonacci p-numbers								
A000930	$1/4$	$2/6$	$3/9$	$4/13$	$6/19$	$9/28$	0.318	114.5
A003269	$1/5$	$2/7$	$3/10$	$4/14$	$5/19$	$7/26$	0.276	99.2
A003520	$1/6$	$2/8$	$3/11$	$4/15$	$5/20$	$6/26$	0.245	88.2
A005708	$1/7$	$2/9$	$3/12$	$4/16$	$5/21$	$6/27$	0.222	79.9

TABLE 6. Derivation of Divergence Angles from Ratios of Linear Expressions.

OEIS #						Divergence Angle	Degrees
Common Fibonacci Numbers							
A000045	$1/(q+2)$	$(q+1)/(2q+3)$	$(q+2)/(3q+5)$	$(2q+3)/(5q+8)$	$(3q+5)/(8q+13)$	0.381	137.5
A000032	$1/(q+3)$	$(q+1)/(3q+4)$	$(q+2)/(4q+7)$	$(2q+3)/(7q+11)$	$(3q+5)/(11q+18)$	0.276	99.36
A000285	$1/(q+4)$	$(q+1)/(4q+5)$	$(q+2)/(5q+9)$	$(2q+3)/(9q+14)$	$(3q+5)/(14q+23)$	0.217	78
A022095	$1/(q+5)$	$(q+1)/(5q+6)$	$(q+2)/(6q+11)$	$(2q+3)/(11q+17)$	$(3q+5)/(17q+28)$	0.178	64.1
A022096	$1/(q+6)$	$(q+1)/(6q+7)$	$(q+2)/(7q+13)$	$(2q+3)/(13q+20)$	$(3q+5)/(20q+33)$	0.151	54.4
A022097	$1/(q+7)$	$(q+1)/(7q+8)$	$(q+2)/(8q+15)$	$(2q+3)/(15q+23)$	$(3q+5)/(23q+38)$	0.131	47.25
Anomalous Fibonacci Numbers							
A001060	$1/(3-q)$	$(q+1)/(3q+2)$	$(q+2)/(2q+5)$	$(2q+3)/(5q+7)$	$(3q+5)/(7q+12)$	0.419	151.14
A022113	$(2-q)/5-3q$	$(2q+1)/(5q+2)$	$(q+3)/(2q+7)$	$(3q+4)/(7q+9)$	$(4q+7)/(9q+16)$	0.439	158.15
A022114	$(3-2q)/7-5q$	$(3q+1)/(7q+2)$	$(q+4)/(2q+9)$	$(4q+5)/(9q+11)$	$(5q+9)/(11q+20)$	0.451	162.42
Fibonacci p-numbers							
A000930	$1/(q+3)$	$(q+1)/(2q+4)$	$(q+2)/(3q+6)$	$(q+3)/(4q+9)$	$(2q+4)/(6q+13)$	0.318	114.5
A003269	$1/(q+4)$	$(q+1)/(2q+5)$	$(q+2)/(3q+7)$	$(q+3)/(4q+10)$	$(q+4)/(5q+14)$	0.276	99.2
A003520	$1/(q+5)$	$(q+1)/(2q+6)$	$(q+2)/(3q+8)$	$(q+3)/(4q+11)$	$(q+4)/(5q+15)$	0.245	88.2
A005708	$1/(q+6)$	$(q+1)/(2q+7)$	$(q+2)/(3q+9)$	$(q+3)/(4q+12)$	$(q+4)/(5q+16)$	0.222	79.9

*Note: Corresponding terms of these series for the common and anomalous Fibonacci series are in the ratio $1/(q+1)$, so that the ratios will tend to converge to this limit (see Appendix). "q" values for Common & Anomalous Fibonacci series: q=0.618034; "q" values for Fibonacci p-number series: for A000930, $q = 0.682328$; for A003269, $q = 0.724491$; for A003520, $q = 0.754877$; for A005708, $q = 0.778059$.

TABLE 7. Summary of the Fibonacci Circle Patterns.

	Stem Cell Niche Size	Rules for Asymmetric Cell Division		
OEIS #	Number of Initiating Cells*	Maturation Delay (# cycles)	Number of Divisions per Dividing Cell	Number of Cycles Before Direction of Cell Division Alternates
Common Fibonacci Numbers				
A000045	3	1	2	1
A000032	4	1	2	1
A000285	5	1	2	1
A022095	6	1	2	1
A022096	7	1	2	1
A022097	8	1	2	1
Anomalous Fibonacci Numbers				
A013655	2	1	variable	1
A022113	2	1	variable	1
A022114	2	1	variable	1
Fibonacci p-numbers				
A000930	4	2	3	2
A003269	5	3	4	3
A003520	6	4	5	4
A005708	7	5	6	5
*Note: Number of cells in the stem cell niche is the number of initiating cells that are present before two or more cells divide in a single time cycle.				

6. DISCUSSION

Modeling age-structured Fibonacci circle patterns shows that specific rules produce the known Fibonacci number patterns in terms of the number sequence and divergence angle. Indeed, model output patterns fit the common, anomalous, and p-number Fibonacci sequences and divergence angles. The differences between the various Fibonacci number series were derived by introducing perturbations in model rules including number of initiating cells, limit in number of cell divisions, order of cell division, direction of cell division, and delay in maturation. Incorporation of these rules into the model generated a unique Fibonacci circle pattern that fit each of the known Fibonacci number series and divergence angles. Namely, the number of cells that sequentially occurred at each time period fit the different Fibonacci number series. Moreover, growth of the Fibonacci circles occurred circumferentially and not from a single point in the circle's center or circumference. This circumferential growth resembles the manner whereby circular structures develop in nature. It also resonates with the process of tissue renewal wherein cell division is continually occurring within the tissue itself while the organization of cells in the tissue stays the same.

Modeling also shows that the size of the stem cell niche (based on the number of initiating cells) affects Fibonacci organization and structure. Clearly, modeling shows that once the stem cell niche is formed, it provides a foundation on which the growth of the circle occurs according to the rules outlined by Parkinson's law. Indeed, modeling the common Fibonacci numbers shows that specific Fibonacci circle patterns emerge based on different stem cell niche sizes even though rules for cell division were the same after the stem cell niche had formed. Moreover, it was observed that a linear relation exists between the stem cell niche size and the magnitude of the divergence angle.

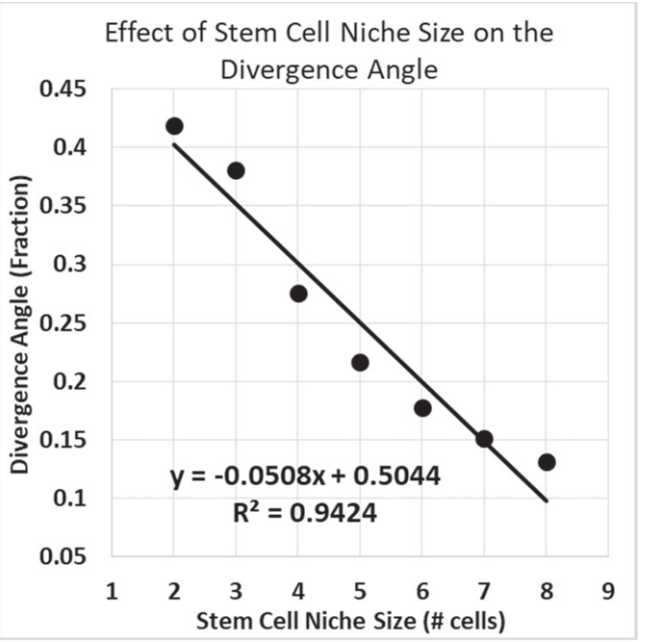

FIGURE 9. The plot shows the linear relation between the stem cell niche size and the divergence angle for the six common Fibonacci number series and the anomalous Fibonacci sequence A001060.

However, the size of the stem cell niche is not the only factor that affects the structure of the age-structured pattern. Indeed, modeling the anomalous Fibonacci number patterns shows that the number of initiating cells is the same, but the rules for cell division are variable within the time period after the stem cell niche has formed. This result reveals that differences in specific rules for cell division can lead to differences in the organizational patterns of Fibonacci circles. Thus, this finding indicates that differences in the mode of cell division can lead to differences in tissue organization.

For the Fibonacci p-number series, modeling also shows that changes occur in both stem cell niche size and the mode of cell division. Indeed, the number of initiating cells was different among the different Fibonacci p-number age-structure patterns. The rules for cell division differed in terms of maturation delay before immature cells divide, number of divisions per dividing cell, and number of cycles before the direction of cell division also occurs. Clearly, these differences in stem cell niche size and rules for cell division affect the rate of system growth (Fibonacci circle expansion) based on cell numbers at different time points which correlate with the Fibonacci p-number series.

Once specific age-based structures were determined that fit each of the different Fibonacci number sequence patterns, it was shown that the angle of divergence can be derived from the modeling results in terms of the number of cells at successive time cycles and from ratios of the linear expressions. Thus, modeling shows that both the specific mode of cell division and the size of the stem cell niche determine the degree of the divergence angle.

7. Summary and Conclusions

Modeling age-structured Fibonacci circle pattern formation indicates that specific biological rules lead to the different Fibonacci structures in nature. Indeed, specific patterns emerged from modeling that fit known Fibonacci number sequences and associated divergence angles. For example, the order of cell division was determined that corresponds to the generalized Fibonacci series (A000045) and that generates a Fibonacci circle with a divergence angle of 137.5 degrees (see Figure 1). Model output patterns also fit with the other common, anomalous, and Fibonacci p-number series and divergence angles. The different Fibonacci number patterns occurred according to differences in stem cell niche size and rules for the mode of asymmetric cell division (summarized in Table 7). That specific age-structured Fibonacci circle patterns fit different Fibonacci sequences indicates that a simple set of rules controls the formation of tissue structure and organization in plants and animals. Thus, studying Fibonacci circle patterns reveals that the mechanism underlying the organization of biological tissues involves specific age-structure rules for cell division and maturation in each tissue. The important finding from this study is that biological rules for specific modes of asymmetric cell division and stem cell niche size are determinants of tissue organization in nature. This finding not only has significance for understanding the rules of life for the organization of healthy tissues but also for understanding mechanisms in wound healing and diseases, such as cancer and birth defects, which arise from tissue disorganization.

APPENDICES

Appendix A. Geometric Expression of the Fibonacci p-numbers

The Fibonacci p-numbers are often expressed geometrically.

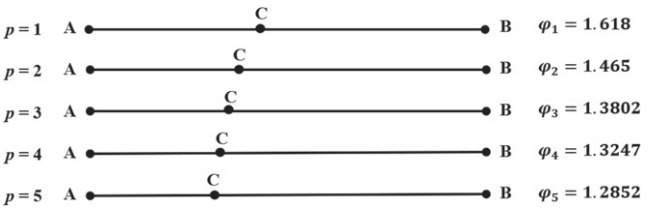

The Golden p-ratio is the ratio of two quantities CB and AC if their ratio is the same as the ratio of two larger quantities AB and CB raised to the power p. Algebraically, for AB, CB, and AC with $AB > CB > AC$, the ratio is:

$$\varphi_p = \frac{CB}{AC} = \left(\frac{AB}{CB}\right)^p,$$

where the Greek letter (φ_p) represents the Golden p-ratio [13, 26]. It is also the positive root that is a solution to the quadratic equation:

$$\varphi_p^{p+1} - \varphi_p^p = 1.$$

The Fibonacci p-numbers, denoted F_p, are a generalization of the well-known Fibonacci numbers. Fibonacci p-numbers form a sequence, the Fibonacci p-sequence

(Table 1), whereby each number is the sum of two preceding ones based on the recursive relation for $n > p + 1$:

$$F_p(n) = F_p(n-1) + F_p(n-p-1),$$

with $F_p(0) = 0$, and $F_p(1) = F_p(2) = \cdots = F_p(p) = F_p(p+1) = 1$.

Fibonacci *p*-numbers are closely linked to the Golden *p*-ratio. For *p* = 1, this represents the Fibonacci sequence, and the Fibonacci numbers are related to the classic Golden ratio. The Binet formula gives the *n*th Fibonacci number in terms of *n* and the Golden ratio [13, 26]. It designates that as *n* increases, the ratio of two consecutive Fibonacci numbers tends to the Golden ratio:

$$F_n = \frac{\varphi^n - \psi^n}{\varphi - \psi} = \frac{\varphi^n - \psi^n}{\sqrt{5}},$$

where $\varphi = \frac{1+\sqrt{5}}{2} \approx 1.618034$ and $\psi = \frac{1-\sqrt{5}}{2} \approx 0.618034$.

A generalized Binet formula for Fibonacci *p*-numbers was derived by Kilic [13] and Stakhov [26].

Appendix B. Parkinson's Law

Parkinson's Law for the growth of staff in a bureaucracy and expansion of committees states the following rules [9].

1. The first member shall retire or become an advisory member after one year. Every other member shall serve as a voting member for exactly two years and shall then retire or else continue to serve but as an advisory member.
2. In each year of service, each voting member shall nominate one new member to the committee.
3. Each member shall have a rank number according to the seniority of appointment. Rank 1 will be given to the first member and 2, 3, 4, ... to the other members as they are appointed. Members shall retain this rank after retirement.
4. Voting members shall appoint new members in strict order of seniority.
5. In years of even dates, new members shall take their seats at the committee table on the left of the member appointing them. In odd years, they shall be seated on the right of their sponsors.
6. An advisory member shall continue to attend meetings of the planning committee. If unable to do so owing to pressure from work on other committees to which they belong, they shall automatically be appointed to the rank of retired member.

Appendix C. Expansion of the Geometric Progressions as a Function of (*q* + 1)

It has been observed that the reciprocal (termed the quotient q) of the Golden *p*-ratio (i.e., $q = \frac{1}{\varphi_p}$) is key to the Fibonacci *p*-numbers [5].

As $\varphi^{p+1} = \varphi^p + 1$ (mentioned in Appendix A), using $\varphi = \frac{1}{q}$, we get on dividing by φ^p, the equation $\varphi = 1 + \frac{1}{\varphi^p}$, so $\varphi = 1 + q^p$, or $\frac{1}{q} = 1 + q^p$, which gives $1 = q + q^{p+1}$.

So, for *p* = 1, this geometric expression can be written as $\frac{q}{1-q} = \frac{1}{q}$ so $q^2 = 1 - q$.

Based on this expression, the expansion of the geometric progressions for the growth of the Fibonacci circles as a function of time is obtained by the following simple approach [9].

TABLE C.1. Expressions for Cell Division as a Function of $(q+1)$.

$(q+1)^5$	$5q+8$
$(q+1)^4$	$3q+5$
$(q+1)^3$	$2q+3$
$(q+1)^2$	$q+2$
$(q+1)$	$q+1$
q	q
1	1
q^2	$-q+1$
q^3	$2q-1$
q^4	$3q+2$
q	$5q-3$

The term $(q+1)$ raised to the second power can thus be simplified as follows:

$$(q+1)^2 = q^2 + 2q + 1.$$

Since $q^2 = 1 - q$, then substituting back in for q^2,

$$(q+1)^2 = q + 2.$$

The term $(q+1)$ raised to the third power can then be simplified as follows:

$$(q+1)^3 = (q+1)(q+1)^2.$$

Since $(q+1)^2 = q+2$, then substituting back in for $(q+1)^2$,

$$(q+1)^3 = 2q + 3.$$

Using this same approach in a repetitive manner, the terms in the geometric progression can be derived as a function of powers of $(q+1)$.

Similarly, for Fibonacci *p*-number sequences, the *p*-ratio is $\frac{q}{1-q} = \left(\frac{1}{q}\right)^n$, so $q^{n+1} = 1 - q$, where $n = p$ [5]. For example, when $p = 2$, $q^3 = 1 - q$.

TABLE C.2. Expressions for Geometric Progression as a Function of $(q+1)$.

Fibonacci *p*-number	Expression	*q*-value ($q = \frac{1}{\varphi_p}$)
$p = 1$	$q^2 = 1 - q$	0.618034
$p = 2$	$q^3 = 1 - q$	0.682327
$p = 3$	$q^4 = 1 - q$	0.724491
$p = 4$	$q^5 = 1 - q$	0.754877
$p = 5$	$q^6 = 1 - q$	0.778089

ACKNOWLEDGMENTS

A special thank you to Dr. Gilberto Schleiniger and members of the research team in the Center for Applications of Mathematics in Medicine at the University of Delaware for their strong support and enlightening discussions. Great appreciation to Dr. Nicholas Petrelli and The Cawley Center for Translational Cancer Research for programmatic

support. Also, Dr. Jeremy Z. Fields is acknowledged for assistance with scientific writing and Ryan M. Boman for helpful discussions.

Disclosure Statement

The author reported no potential conflict of interest.

Funding

This work was funded in part by generous support from The Lisa Dean Mosley Foundation for Stem Cell Research, BioCode Innovations Inc., and CATX Inc.

Orcid

Bruce M. Boman http://orcid.org/0000-0002-1335-9149

References

[1] Adler, I. (1974). A model of contact pressure in phyllotaxis. *J. Theor. Biol.* 45: 1–79.
[2] Affolter, M., Bellusci, S., Itoh, N., Shilo, B., Thiery, J. P., Werb, Z. (2003). Tube or not tube: remodeling epithelial tissues by branching morphogenesis. *Dev Cell* 4: 11–18.
[3] Andrew, D. J., Ewald, A. J. (2010). Morphogenesis of epithelial tubes: insights into tube formation, elongation, and elaboration. *Dev Biol*. 341: 34–55.
[4] Berdyshev, A. P. (1972). On some mathematical regularities of biological processes. *Zhurnal Obshchebiologii* 33: 631–638.
[5] Boman, B. M. (2020). Geometric Capitulum Patterns based on Fibonacci *p*-proportions. *Fibonacci Quart.* 58(5): 91–102.
[6] Boman, B. M., Dinh, T. N., Decker, K., Emerick, B., Raymond, C., Schleiniger, G. (2017). Why do Fibonacci numbers appear in patterns of growth in Nature? A model for tissue renewal based on asymmetric cell division. *Fibonacci Quart.* 55: 30–41.
[7] Boman, B. M., Yihan, Y., Decker, K., Raymond, C., Schleiniger, G. (2019). Geometric branching patterns based on *p*-Fibonacci sequences: self-similarity across different degrees of branching and multiple dimensions. *Fibonacci Quart.* 57(5): 29–41.
[8] Galis, F., van Alphen, J. J. M., Metz, J. A. J. (2001). Why do most species have five digits on their hands and feet? *Trends Ecol. Evol.* 16: P637–646.
[9] Holland, J. M. (1972). *Studies in Structure*. London: Macmillan Press LTD.
[10] Impens @ Valvas, C. (2022). Most rare: Mathematical proof of the golden angle. Available at: https://ci47.blogspot.com/2018/04/most-rare-mathematical-proof-of-golden.html, Accessed July 26, 2022.
[11] Jean, R. J. (1994). *Phyllotaxis: A Systemic Study in Plant Morphogenesis*. Cambridge: Cambridge University Press, pp. 31–47.
[12] Jean, R. V. (1981). An L-system approach to nonnegative matrices for the spectral analysis of discrete growth functions of populations. *Math. Biosci.* 55: 155–168.
[13] Kilic, E. (2008). The Binet formula, sums and representations of generalized Fibonacci *p*-numbers. *Eur. J. Combin.* 29: 701–711.
[14] Knott, R. (2022). Fibonacci numbers and nature. Web resource available at http://www.maths.surrey.ac.uk/hosted-sites/R.Knott/Fibonacci/fibnat.html, Accessed July 26, 2022.
[15] Lindenmayer, A. (1978). Algorithms for plant morphogenesis. *Acta Biotheoretica* 27: 37–82.
[16] Luck, H. B. (1975). Elementary behavioural rules as a foundation for morphogenesis. *J. Theoret. Biol.* 54: 23–34.
[17] Negishi, R., Sekiguchi, K., Totsuka, Y., Uchida, M. (2017). Determining parastichy numbers using discrete Fourier transforms. *Forma* 32: 19–27.

[18] Okabe, T. (2016). The riddle of phyllotaxis: exquisite control of divergence angle. *Acta Soc. Bot. Pol.* 85: 3527. DOI: 10.5586/asbp.3527

[19] Pennisi, E. (2018). The momentous transition to multicellular life may not have been so hard after all. *Science*. Available at https://www.science.org/content/article/momentous-transition-multicellular-life-may-not-have-been-so-hard-after-all.

[20] Richards, F. J. (1951). Phyllotaxis: Its quantitative expression and relation to growth in the apex. *Phil. Trans. R Soc. London B* 235: 509–564.

[21] Ridley, J. N. (1982). Packing efficiency in sunflower heads. *Math. Biosci.* 58: 129–139.

[22] Rozin, B. (2020). *Double Helix of Phyllotaxis: Analysis of the Geometric Model of Plant Morphogenesis*. Irvine: Brown Walker Press/Universal Publishers, Inc.

[23] Shipman, P., Sun, Z., Pennybacker, M., Newell, A. C. (2011). How universal are Fibonacci patterns? *Eur. Phys. J. D.* 62: 5–17.

[24] Spears, C. P., Bicknell-Johnson, M. (1998). Asymmetric cell division: Binomial identities for age analysis of mortal vs. immortal trees. *Applic Fibonacci Numbers* 7: 377–391.

[25] Spears, C. P., Bicknell-Johnson, M., Yan, J. (2009). *Fibonacci Phyllotaxis by Asymmetric Cell Division: Zeckendorf and Wythoff Trees*. Winnipeg: Utilitas Mathematica Publishing, pp. 257–272.

[26] Stakhov, A. P., Olsen, S. (2009). *The Mathematics of Harmony: From Euclid to Contemporary Mathematics and Computer Science.* Hackensack: World Scientific Publishing.

[27] Stewart, I. (2011). Florally finding Fibonacci. In: *The Mathematics of Life*. New York: Basic Books, pp. 38–55.

[28] Varney, R. M., Speiser, D. I., Cannon, J. T., Aguilar, M. A., Eernisse, D. J., Oakley, T. H. (2024). A morphological basis for path-dependent evolution of visual systems. *Science* 383: 983–987. DOI: 10.1126/science.adg2689.

[29] Wundrak, S., Paul, J., Ulrici, J., Hell, E., Rasche, V. (2015). A small surrogate for the golden angle in time resolved radial MRI based on generalized Fibonacci sequences. *IEEE Trans. Med. Imaging* 34: 1262–1269.

MSC2020: 11B39, 33C05

Center for Applications of Mathematics in Medicine, Department of Mathematical Sciences, University of Delaware, Newark, DE 19716, USA
Email address: BrBoman@udel.edu

This article has been republished with minor changes. These changes do not impact the academic content of the article.